EARTHQUAKE ENGINEERING PRACTICE

Nonlinear Rotation of Capacity-Protected Foundations: The 2015 Canadian Building Code

Perry Adebar,[a)] **M.EERI**

When foundations are capacity-protected, inelastic deformations will occur primarily in the seismic force-resisting system. Soil flexibility can be ignored when determining seismic loads, but footings will rotate when subjected to the maximum overturning moment, and this may increase building drifts, particularly in lower stories where gravity-load columns are less flexible. A "hand calculation" method is presented for estimating rotation of a footing from the uniform bearing stress distribution required to resist the applied overturning moment. The method, which has been adopted in the 2015 Canadian building code, accounts for initial linear rotation of footings and additional nonlinear rotation due to footing uplift and nonlinearity of soil. A quick, safe estimate can be made using approximate equations, or a more accurate estimate can be made by determining two parameters from figures. Design examples demonstrate how the method can be used to design foundations for improved performance at a small additional cost. [DOI: 10.1193/012814EQS022M]

INTRODUCTION

When determining seismic loads for the design of a building, it is common practice to ignore the flexibility of the seismic force-resisting system (SFRS) due to soil deformation and simply to assume the SFRS is fixed at the base. The increased stiffness of the SFRS results in higher seismic loads that the SFRS and the supporting foundations are designed to resist. While underestimating foundation flexibility generally gives safe estimates of seismic loads, it may result in unsafe estimates of building displacements. A recent study of shear wall buildings where both shear walls and supporting soil were modeled with nonlinear elements (Bazargani 2014) showed that, as expected, foundation rotations result in reduced bending moment demands on the shear walls, but in increased total building displacements compared to the results from fixed-base models. As maximum interstory drifts near the top of the buildings did not increase much, ignoring soil deformation is often a reasonable design simplification.

Canadian practice has permitted the construction of gravity load–resisting frames that are much less resilient than those normally constructed in the United States. Throughout Canada, including regions of high seismicity, thin walls/piers with much less flexibility about the strong axis of bending are often used in place of square columns that are flexible about

[a)] Dept. of Civil Engineering, The University of British Columbia, Vancouver, BC, Canada, V6T1Z4

Earthquake Spectra, Volume 31, No. 4, pages 1885–1907, November 2015;

both axes, and gravity-load columns and walls usually have very few ties (i.e., minimal confinement; Adebar et al. 2010). Columns and walls are subjected to maximum axial load near the base of the building where foundation rotations have the largest influence on interstory drift demands. Nonlinear analyses of shear walls buildings showed that while fixed-base models suggest very small interstory drifts near the base, more accurate models accounting for footing uplift and soil deformation may reveal significant interstory building drifts at that level. If the gravity load–resisting frame is stiff and brittle, ignoring foundation rotations may be very unsafe.

The next generation of building codes in Canada is tightening the seismic design requirements for gravity-load frames. The 2015 edition of the National Building Code of Canada (2015 NBCC) states that the increased displacements resulting from foundation rotations shall be shown to be within acceptable limits for both the SFRS and gravity-load frame. The 2014 edition of Canadian Standard CSA A23.3, which provides the reinforced concrete design provisions for 2015 NBCC, has adopted the following procedure for capacity-protected foundations: (1) determine seismic loads ignoring footing rotation; (2) design SFRS and foundations for the seismic loads; (3) determine foundation rotation due to an applied overturning moment equal to the overturning capacity of the SFRS; (4) add the rigid body rotation due to foundation rotation to the SFRS deformations due to the seismic loads; and (5) design the gravity-load frame for the resulting total displacements of the building.

Because foundation rotation due to earthquake loading has traditionally been ignored in the design of buildings, simplified methods are not readily available to estimate how much the foundation supporting a single shear wall or an entire shear-wall core of a building will rotate when subjected to an overturning moment. The problem is nonlinear, due to both footing uplifting and the reduction in soil stiffness with strain (nonlinearity of soil). Centrifuge model tests (Gajan et al. 2005) have shown that footing uplift and sliding are coupled, and permanent vertical deformation of the footing accumulates with the number of cycles. Rigorous computer solutions are available for determining the nonlinear rotation of foundations by modeling the soil half-space using finite elements or boundary elements (e.g., Yan and Martin 1999). This is the type of solution that a specialist geotechnical consultant can provide. Simpler solutions have been developed using Winkler spring models of the soil (e.g., Gazetas and Mylonakis 1998), which is a solution that a structural engineer may use for a special study when the spring properties are provided by the geotechnical consultant. Further simplified solutions for determining the moment-rotation response of foundations have been developed (e.g., Allotey and El Naggar 2003, Pender et al. 2013, Bazargani 2014); however these methods are not simplified enough to be adopted into a building code.

The objective of this study was to develop a "hand calculation" method for estimating the rotation of *capacity-protected* foundations from the uniform bearing stress distribution required to resist the applied vertical load and overturning moment. The method has been adopted in 2014 Canadian Standard CSA A23.3. Note that a foundation is *capacity-protected* when the SFRS has a lower overturning capacity than the foundation so that the maximum seismic forces are limited by inelastic action in the SFRS rather than by rocking of the footing.

Trilinear Winkler springs are used to model footing uplift, nonlinearity of soil, and the foundation bearing capacity. The well-known solutions for the linear rotational stiffness of

foundations prior to uplift are used to define the initial stiffness of the Winkler springs; but are converted into a non-dimensional parameter that simplifies the calculation of rotation. The nonlinear bearing stress distributions due to trilinear Winkler springs are converted to statically equivalent uniform bearing stress distributions as structural engineers traditionally assume a uniform bearing stress to design foundations. A non-dimensional parameter is introduced to relate the uniform bearing stress to the soil deformations at the "toe" of the footing accounting for the nonlinearity of soil. The resulting proposed method for estimating the nonlinear rotation of capacity-protected shear wall foundations is simple enough that all calculations can be done without a computer. The method is verified with the results from large-scale experiments. Finally, simplified versions of the method are presented for making quick, safe estimates of foundation rotation for situations where the gravity-load frame can easily tolerate the increased displacements of the building.

THEORY

LINEAR STIFFNESS OF FOOTINGS

Solutions are available for determining the linear rotational stiffness of a footing. ASCE 41-06 (2007) provides solutions adapted from Pais and Kausel (1988) and Gazetas (1991). The linear rotational stiffness of a footing can be expressed in the following general form:

$$K_\theta = \frac{G}{(1-\nu)} \cdot I^{0.75} \cdot A_1 \tag{1}$$

where G = the effective shear modulus of soil; ν = Poisson's ratio of soil; I = the moment of inertia of the bottom surface of the footing in the direction of rotation $I = b_f l_f^3/12$; b_f = width of footing (parallel to axis of rotation); l_f = length of footing (perpendicular to axis of rotation); and A_1 = non-dimensional constant that depends on the footing geometry, such as length-to-width and depth-to-length ratios, and has a range of possible values depending on the solution used to determine K_θ.

If the linear rotational stiffness of a foundation, including contributions from the sides of an embedded footing, is modeled by an infinite number of uniformly spaced vertical Winkler springs acting on the underside of the footing, the stiffness of the springs is calculated by dividing the total rotational stiffness K_θ by the moment of inertia of the bottom surface of the footing I. The force per unit area (bearing stress) per unit vertical deflection of the footing (i.e., the modulus of subgrade reaction) can be expressed as:

$$k_{sv} = \frac{G}{(1-\nu) \cdot l_f} \cdot A_2 \tag{2}$$

where $A_2 = A_1 \cdot (12 l_f/b_f)^{0.25}$ is another non-dimensional parameter that depends on footing geometry and the solution used to determine K_θ. The inverse, which is subgrade flexibility (vertical displacement per unit bearing stress), is needed to determine the rotation of a footing:

$$f_{sv} = 1/k_{sv} = \frac{0.2\xi_L(1-\nu) \cdot l_f}{G} \tag{3}$$

where $\xi_L = A_3 = 1/(0.2A_2)$ is yet another non-dimensional parameter that depends only on the footing geometry and the solution used to determine K_θ. A_3 is given the symbol ξ_L as it will appear in the final solution for determining footing rotation. The 0.2 value was selected so that ξ_L has an upper-bound value of 1.0. The parameter ξ_L can be determined from A_1, A_2, or directly from K_θ:

$$\xi_L = \frac{G \cdot I}{0.2(1-\nu) \cdot l_f \cdot K_\theta} \tag{4}$$

Figure 1 presents the values of ξ_L determined from the rotational stiffness equations given by Gazetas (1991), shown as solid lines, and the equations in ASCE 41-06 (2007), shown as dashed lines. The two sets of equations provide similar results except when the length-to-width ratio of the footing $l_f/b_f = 1.0$. As different equations are used for $l_f/b_f \leq 1.0$ and $l_f/b_f > 1.0$ (four equations were used for Figure 1), there is a discontinuity at $l_f/b_f = 1.0$. The results of the four equations when $l_f/b_f = 1.0$ are shown in Figure 1b. Note that as the subgrade flexibility is proportional to ξ_L (stiffness is inversely proportional to ξ_L), an upper-bound estimate of ξ_L is safe when estimating footing rotation.

The one parameter that appears in the rotational stiffness equations, but that is not shown in Figure 1, is the ratio of footing depth (thickness) d_f to the vertical distance from top of ground to the underside of footing, D_f. This parameter, which reflects the enhancement of friction on the footing sides and radiation damping waves emanating from the footing sides (Gazetas 1991), only has a significant influence when the footing thickness, d_f, is large compared to the footing length. Since the thickness of shear wall foundations is usually small compared to the length, d_f/D_f was taken equal to 1.0 to determine Figure 1. To demonstrate the reduction in footing flexibility (increase in stiffness) that is ignored in Figure 1, the following reductions in ξ_L occur when d_f/D_f is reduced (by a factor of 10) to 0.1 and d_f/l_f is taken equal to 0.1, 0.2, 0.3, and 0.4, respectively: 2%, 6%, 11%, and 14%.

NONLINEAR WINKLER SPRINGS

Figure 2 presents three types of relationships between the bearing stress applied to soil and the corresponding displacement of soil. The curve labeled "L" is a linear elastic spring with constant stiffness, k_{sv}, given by Equation 2. Prior to footing uplifting, such linear elastic springs provide the foundation rotational stiffness given by Equation 1. The bilinear relationship (BL) assumes soil remains linear elastic until reaching a bearing stress equal to q_{ult} at which point the soil yields. The third type of curve shown in Figure 2 is trilinear (TL). When the bearing stress reaches a value of $n \cdot q_{ult}$, the slope of the curve reduces to $m \cdot k_{sv}$ to account for the nonlinearity of the soil stress-strain behavior. Both n and m have values between 0 and 1.0. As in the bilinear relationship, the soil yields when the bearing stress reaches q_{ult}. The curves shown in Figure 2 all have $n = 0.32$, as well as the following values of m (for TL1 to TL5, respectively): 0.50, 0.30, 0.17, 0.08, and 0.04. The value of n was selected so that when $m < 1.0$, it results in trilinear curves with similar shape to the default curve for sand in the QzSimple1 material model in OpenSees, which is consistent with the p-y curves by Boulanger et al. (1999). The default curves for sand were calibrated to the backbone curve recommended by Vijayvergiya (1977). The values for m were selected to give a wide range of curves.

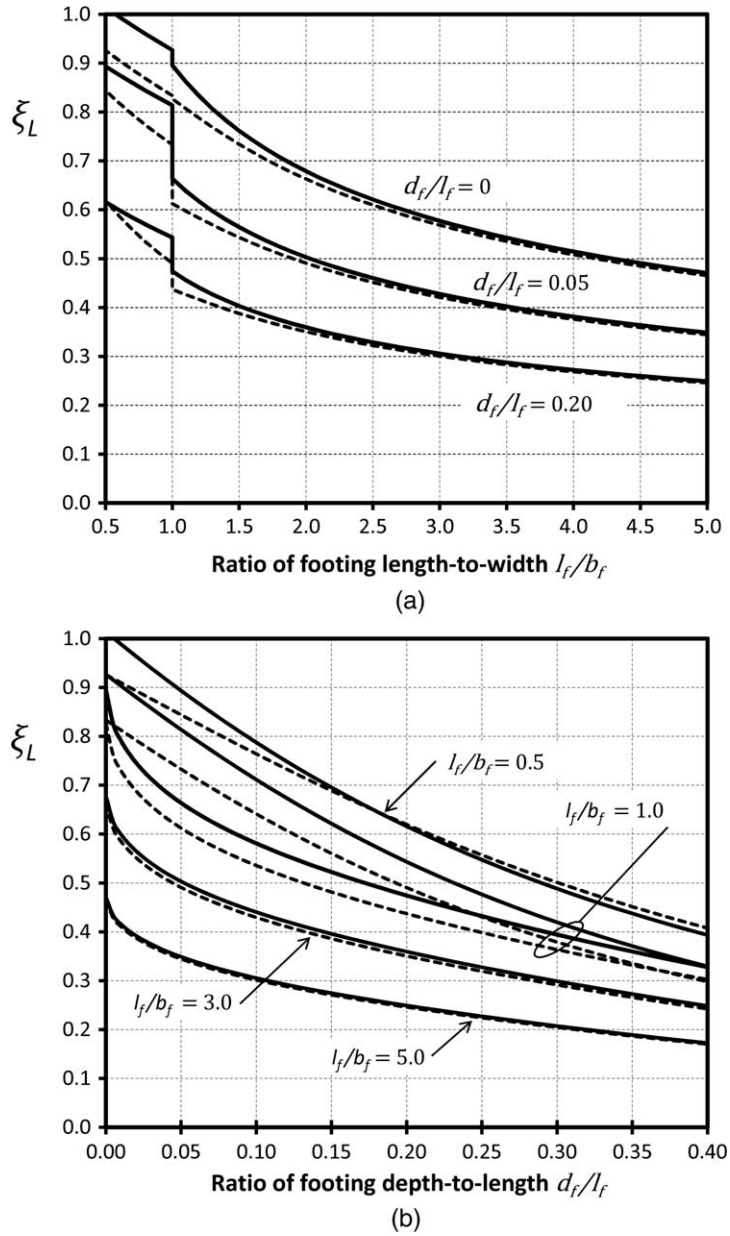

Figure 1. Non-dimensional parameter accounting for footing geometry on initial rotational stiffness.

STATICALLY EQUIVALENT UNIFORM BEARING STRESS

The concept of replacing a nonlinear stress distribution with a statically equivalent uniform stress distribution is well known to structural engineers who commonly use the approach to calculate the flexural capacity of a reinforced concrete member. The approach

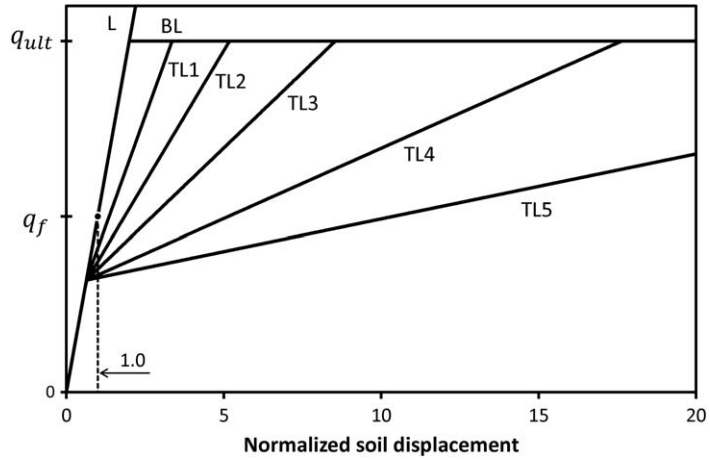

Figure 2. Relationship between bearing stress (vertical axis) and normalized soil displacement defined by different Winkler springs: L = linear, BL = bilinear, TL = trilinear.

is used here to replace non-uniform bearing stress distributions under rotating footings. Figure 3 presents the uniform bearing stress distribution that is statically equivalent to the actual linearly varying bearing stress distribution from a rotating footing supported on linear soil. The actual bearing stress distribution varies from q_{max} at the "toe" of the footing to zero at a distance c from the "toe." To be statically equivalent, the magnitudes and locations of the resultants of the two bearing stress distribution must be equal. The resultant of a linearly varying bearing stress distribution acts at $c/3$ from the "toe" of the footing, thus the length of the statically equivalent uniform bearing stress $\beta c = 2c/3$; or $\beta = 0.667$. The result of the linearly varying bearing stress distribution is equal to the applied vertical load $P = 0.5q_{max} \cdot c \cdot b_f$, while the resultant of the uniform bearing stress distribution is given by: $P = \alpha \cdot q_{max} \cdot 0.667c \cdot b_f$. Thus $q_{unf} = 0.75q_{max}$ or $\alpha = 0.75$. The statically equivalent uniform bearing stress is 75% of the maximum value of the linearly varying bearing stress, or conversely, the maximum bearing stress is $1/0.75 = 1.33$ times the uniform bearing stress.

If the soil remains linear, the maximum displacement at the "toe" of the footing Δ_{max} would be 1.33 times the displacement corresponding to the magnitude of uniform bearing stress. As soil becomes nonlinear, the ratio of maximum bearing stress to uniform bearing stress $(1/\alpha)$ changes, and the ratio of maximum soil displacement to the displacement corresponding to the magnitude of uniform bearing stress will also change. Thus an additional parameter is introduced, which is equal to the ratio of maximum soil displacement at the "toe" of the footing to displacement, corresponding to the magnitude of the uniform bearing stress if soil is in the linear range:

$$\gamma = \frac{\Delta_{max}}{q_{unf}/k_{sv}} \tag{5}$$

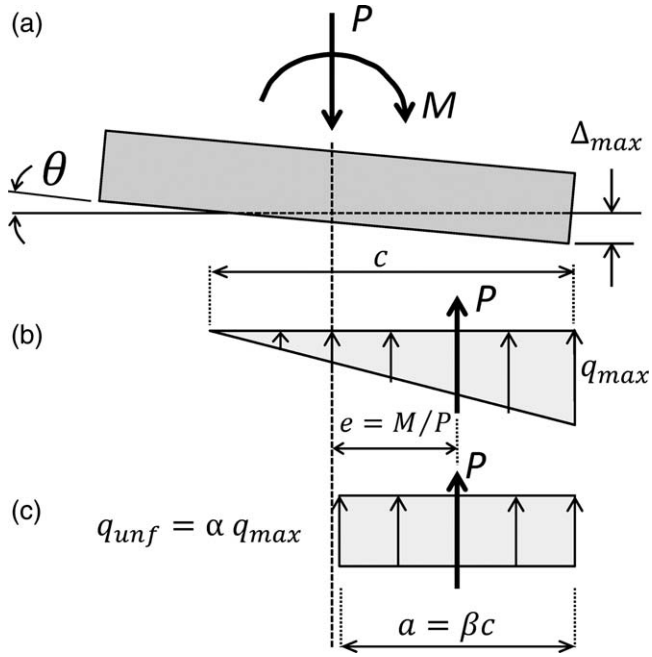

Figure 3. Statically equivalent uniform bearing stress: (a) rotating footing, (b) resulting bearing stress distribution from linear soil, (c) uniform bearing stress with statically equivalent resultant.

If soil is linear, $\Delta_{max} = q_{max}/k_{sv}$ and $\gamma = 1/\alpha = 1.33$. When soil is nonlinear, the parameter γ includes both the increase in soil bearing stress at the "toe" of the footing and the increase in soil displacement due to the nonlinearity of soil.

The nonlinear soil curves shown in Figure 2 can be expressed mathematically in terms of any one bearing stress parameter. An appropriate parameter is the ultimate bearing stress q_{ult}, when soil yields; however, that parameter will typically not be known to the structural engineer. The geotechnical engineer will provide a factored bearing strength, q_f, that includes an appropriate resistance factor. For the design of a foundation to resist the factored overturning moment due to the design earthquake, the Canadian building code suggests a resistance factor of 0.5 and in that case, $q_f = 0.5q_{ult}$. Throughout the current paper $q_f = 0.5q_{ult}$ is used as the parameter defining the nonlinearity of soil. The results and methods presented here can be used with other factors of safety by adjusting q_f accordingly.

Figure 4 summarizes α, β, and γ, which were determined using the six soil springs shown in Figure 2. The parameters are plotted versus the equivalent uniform bearing stress, q_{unf}, as a ratio of the factored bearing strength, q_f. Note that q_{unf} will typically be equal to q_f (i.e., $q_{unf}/q_f = 1.0$) when the foundation is subjected to the factored overturning moment. Bazargani (2014) used an equivalent uniform bearing stress approach for different Winkler springs and used a different definition of γ. He did not include the initial linear response of soil in his solution.

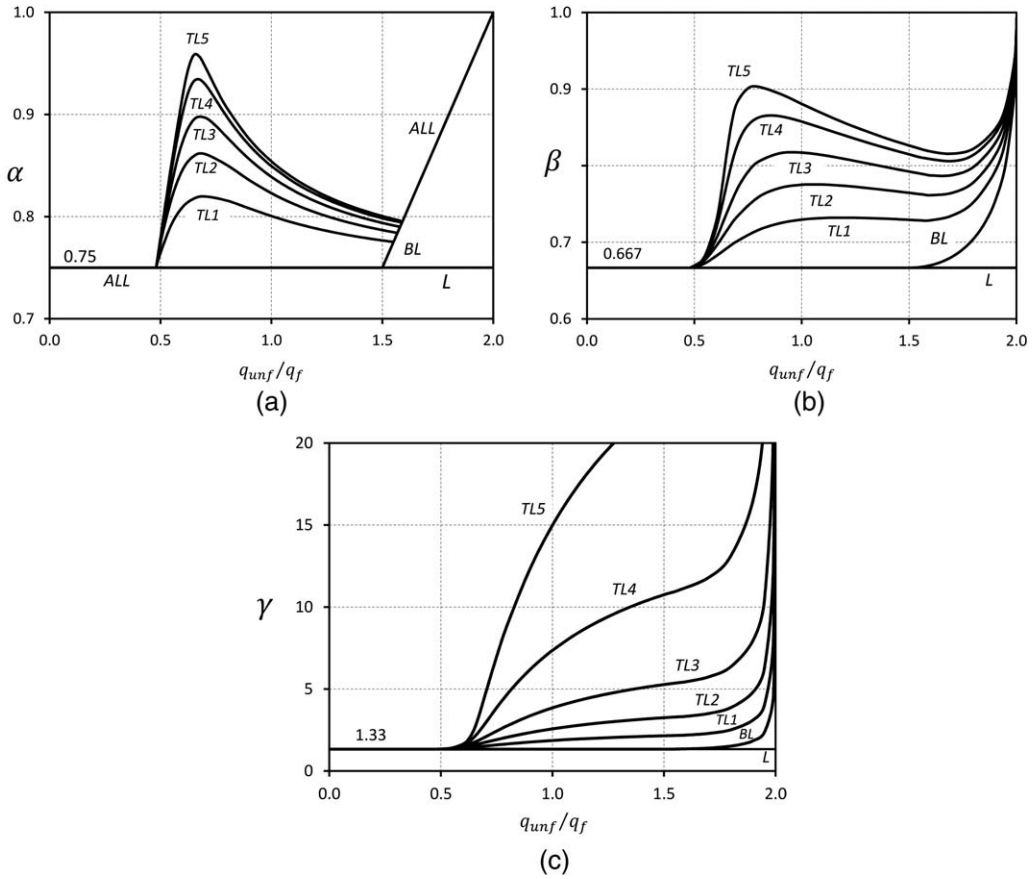

Figure 4. Parameters defining the statically equivalent uniform bearing stress distribution for different Winkler springs: (a) α = ratio of uniform bearing stress to maximum actual bearing stress, (b) β = ratio of uniform bearing stress length to actual bearing stress length, (c) γ = ratio of maximum soil displacement to displacement of linear soil subjected to uniform bearing stress.

EQUILIBRIUM

As structural engineers commonly assume a uniform bearing stress equal to the factored bearing strength, the following two equilibrium equations that relate a uniform soil bearing stress distribution to the applied vertical load, P, and overturning moment, M, are well known:

$$P = q_{unf} \cdot a \cdot b_f \tag{6}$$

$$M = 0.5\ P \cdot l_f(1 - a/l_f) \tag{7}$$

These two equations can be combined into the following single equilibrium equation:

$$M = 0.5\ P \cdot l_f \left\{ 1 - \frac{P/(b_f \cdot l_f)}{q_{unf}} \right\} \tag{8}$$

When designing a footing, the footing width, b_f, parallel to the axis of rotation and footing length, l_f, perpendicular to the axis of rotation are chosen so that the overturning resistance given by Equation 8 is greater than or equal to the applied overturning moment given the applied vertical load, P, and assuming the uniform bearing stress, q_{unf}, is equal to the factored bearing strength, q_f. When the bearing stress $P/(b_f \cdot l_f)$ due to a concentric vertical load (no overturning moment) is small compared to the factored bearing strength, q_f, the overturning resistance of the footing approaches $0.5P \cdot l_f$ as the resultant of the bearing stress is close to the "toe" of the footing.

When the task is to determine the rotation of a foundation with known dimensions b_f and l_f subjected to an applied vertical load, P, and overturning moment, M, Equations 6 and 7 can be rearranged to determine the required uniform bearing stress distribution:

$$a = l_f - 2M/P \tag{9}$$

$$q_{unf} = P/(a \cdot b_f) \tag{10}$$

FOUNDATION ROTATIONS

AFTER FOOTING UPLIFT

Rotation of a foundation subjected to an overturning moment at least as large as the moment to cause the bearing stress at one end of the footing to reduce to zero is given by:

$$\theta = \Delta_{max}/c \tag{11}$$

See Figure 3. Substituting for Δ_{max} from Equation 5 and expressing the soil compression strain length, c, in terms of the uniform stress block length, a, gives:

$$\theta = \frac{\gamma \cdot q_{unf}/k_{sv}}{a/\beta} \tag{12}$$

Replacing $\beta \cdot \gamma$ with $0.89\xi_{NL}$, where ξ_{NL} is a new non-dimensional parameter and 0.89 was chosen so that $\xi_{NL} = 1.0$ when soil is linear; substituting for $1/k_{sv}$ from Equation 3; and, assuming the effective shear modulus, G, is equal to 50% of the initial shear modulus, G_0, gives:

$$\theta = 0.18(1 - \upsilon)\left(\frac{q_{unf}}{0.5G_0}\right)\left(\frac{l_f}{a}\right)\xi_L \cdot \xi_{NL} \tag{13}$$

The third and fourth terms in Equation 13 are the ratios of numbers with the same units so that each term is non-dimensional. The 50% reduction on G_0 is shown in the denominator of the third term to facilitate adjustment of this factor where appropriate. ξ_L is a non-dimensional

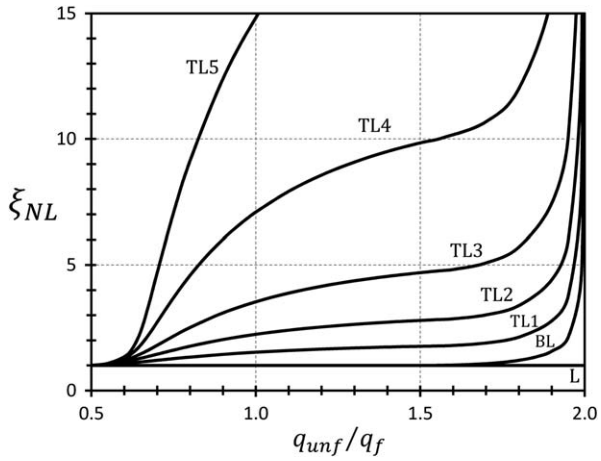

Figure 5. Non-dimensional parameter accounting for increased rotations due to nonlinearity of soil resulting from different Winkler springs.

linear stiffness parameter given in Figure 1. The new non-dimensional parameter that accounts for nonlinearity of soil in compression $\xi_{NL} = 1.124\beta \cdot \gamma$ is equal to 1.0 when the soil is in the linear range and increases as the soil becomes more nonlinear. Figure 5 presents ξ_{NL} for the six trilinear Winkler springs in Figure 2. Equation 13 gives footing rotation in units of radians.

PRIOR TO FOOTING UPLIFT

The minimum overturning moment to cause the bearing stress at one end of the footing to reduce to zero, and the corresponding maximum length of uniform bearing stress, are given by:

$$M \geq 0.5\ P \cdot l_f(1-\beta) \tag{14}$$

$$a \leq \beta \cdot l_f \tag{15}$$

As the minimum value of β is 0.667, the following are safe limits for footing uplift:

$$M \geq P \cdot l_f/6 \tag{16}$$

$$a \leq 0.667 l_f \tag{17}$$

When either Equation 16 or Equation 17 is satisfied, Equation 13 can be used to calculate footing rotation. When the applied overturning moment is less than that given by Equation 16, the foundation rotation can be estimated by assuming the moment-rotation relationship varies linearly from zero at $M = 0$, to the rotation given by Equation 13 when $M = P \cdot l_f/6$. If the soil is linear at footing uplift, this linear interpolation will be exact; while if the soil becomes nonlinear prior to footing uplift, the linear interpolation will be safe (gives larger rotations

than actual). As footing rotations are usually small prior to footing uplift, the linear interpolation method described above is recommended for practice, and this approach has been adopted in the Canadian building code CSA A23.3-2014. Further refined calculations are possible, as described below.

REFINED CALCULATIONS FOR PRIOR TO FOOTING UPLIFT

The soil will be in the linear elastic range at footing uplift if the concentrically applied vertical load, P, causes a uniform bearing stress equal to or less than 50% of the linear bearing stress limit. For the proposed trilinear Winkler springs (Figure 2), the linear elastic limit is $nq_{ult} = 2nq_f = 0.64q_f$. Thus the soil will be in the linear elastic range at footing uplift if:

$$P \leq 0.32\ q_f \cdot b_f \cdot l_f \tag{18}$$

If the soil is in the nonlinear range prior to footing uplift, a more refined estimate of footing rotation than the simplified procedure above can be made. First, the point of footing uplift can be determined using Equation 14. As $\beta \geq 0.667$, the overturning moment will be less than that given by Equation 16. The uniform bearing stress, q_{unf}, at footing uplift is given by Equation 10, with $a = \beta \cdot l_f$, while β depends on q_{unf} and can be determined from Figure 4. Thus an iterative solution is needed: assume β, calculate q_{unf}, calculate β, and repeat until assumed value equals calculated value.

The second possible refinement is to determine the linear response of the footing up until the maximum bearing stress at the "toe" of the footing is equal to the linear elastic limit of $0.64q_f$ for the assumed trilinear Winkler springs, and then use linear interpolation from that point to footing uplift. Figure 6b, which is discussed in the next section in comparison with experimental results, shows an example of this approach (EL = end of linear elastic range and UL = uplift of footing). The overturning moment at the end of the linear elastic range can be calculated using traditional linear mechanics and the rotation can be calculated from Equation 1, or the statically equivalent bearing stress approach can be used. When the soil is in the linear elastic range prior to footing uplift, the bearing stress distribution can be divided into a uniform portion and a linearly varying portion that is zero at one end. The resultant of the linearly varying portion of the bearing stress distribution is equal to the applied overturning moment and a portion of the applied vertical load given by:

$$P^* = (0.64\ q_f \cdot b_f \cdot l_f) - P \tag{19}$$

If P^* is less than 0, the soil is in the nonlinear range prior to the application of an overturning moment. As the bearing stress due to P^* and the applied overturning moment varies linearly from zero at one end, similar to the uplift point, the applied overturning moment can be calculated using Equation 16 with P replaced by P^*. The rotation of the footing in the linear elastic range can be determined from Equation 13 using a and q_{unf} determined from Equations 9 and 10, with P replaced by P^*.

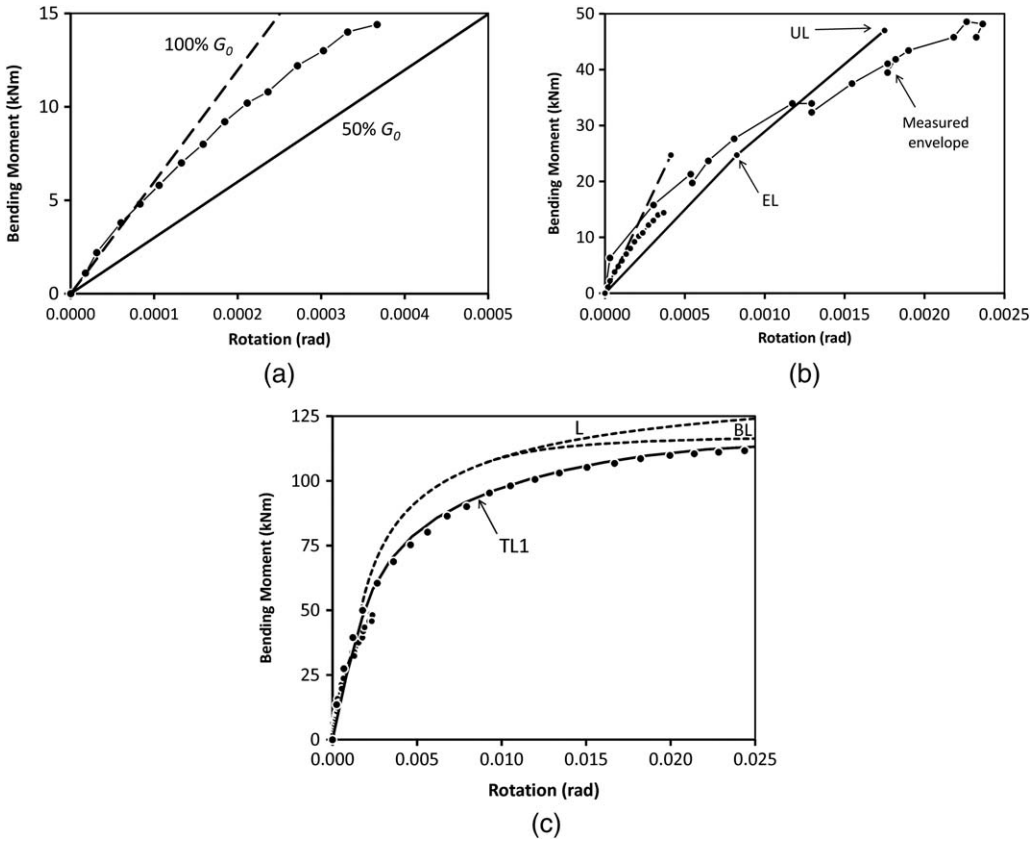

Figure 6. Comparison of predicted and observed rotations from tests of square footings on sand: (a) envelope of small-amplitude force-controlled cycles, (b) envelope of earthquake time history, (c) envelope of increasing cycles until overturning capacity. Laboratory data from Negro et al. (1998).

COMPARISON WITH EXPERIMENTAL RESULTS

SQUARE FOOTINGS ON SAND

Negro et al. (1998) conducted laboratory tests of footings on sand. They subjected a 1 m square footing to a constant vertical load while subjecting the footing to three phases of reverse cyclic overturning moment: Phase I, small-amplitude force-controlled cycles; Phase II, earthquake time history; Phase III, increasing rotations until reaching the overturning capacity.

The soil sample was constructed by pluvial deposition of uniform coarse-to-medium silica sand in a 4.6 m × 4.6 m × 4.0 m deep box. After reconstituting 3 m of sand, a 1 m square footing was constructed by casting a steel plate on top of a layer of concrete mortar. A steel box was then placed outside the foundation, and an additional 1 m of sand was

reconstituted to create an overburden of 20 kPa. To achieve a high degree of saturation, de-aerated water was flushed into the soil box for three days. Two series of tests were performed on two different density deposits; but only the results from the higher density sample are discussed here. The constant vertical load applied on the 1 m square footing bearing on the 85% relative density sand was 300 kN.

The soil properties that are needed to make a prediction of the foundation rotation using Equation 13 are the factored bearing strength, Poisson's ratio and initial shear modulus. The ultimate bearing strength can be determined from the measured overturning capacity of the footing, which was about 118 kNm. Rearranging Equation 8 and solving for $q_{unf} = q_{ult}$ gives $q_{ult} = 1{,}400$ kPa. The factored bearing strength $q_f = 0.5q_{ult} = 700$ kPa. The factored overturning capacity of the footing (what the footing would presumably be designed for) is 86 kNm. The Poisson's ratio, ν, of the saturated sand was assumed to be 0.3.

The initial shear modulus, G_0, was determined to be 90,000 kPa in three ways. First, G_0 can be estimated from measured shear wave velocities using the following well-known relationship:

$$G_0 = \rho \cdot V_s^2 \tag{20}$$

where if the density of the soil ρ has units of kg/m^3, and the shear wave velocity V_S has units of m/s, G_0 will have units of Pa (N/m^2). Using an array of installed geophones, Negro et al. (1998) measured the shear wave velocities at three different vertical positions in the sand. Using an average density of 2,281 kg/m^3 and a shear wave velocity of 200 m/s consistent with the measurements results in $G_0 = 90{,}000$ kPa. The measured initial rotational stiffness of the footing can be used to back-calculate G_0. As the footing is square ($l_f/b_f = 1.0$) and the sides of the footing were not embedded ($d_f = 0$), $\xi_L = 0.895$ from Figure 1. The initial rotational stiffness of the footing for $M \leq 6$ kNm was 60,000 kNm (see Figure 6a). Rearranging Equation 4 and solving for $G = G_0$ gives $G_0 = 90{,}000$ kPa. Allotey and El Naggar (2003) used an empirical expression developed from triaxial tests on the same sand to estimate the small-strain shear modulus, G_o. They found that using an effective stress due to both overburden and applied stresses, and calculating the effective stress at a depth of 1.5 times the equivalent radius of the footing, resulted in $G_0 = 90{,}000$ kPa.

With the three soil parameters ($G_0 = 90{,}000$ kPa, $q_f = 700$ kPa and $\nu = 0.3$) and the non-dimensional parameter defining initial footing rotational stiffness ($\xi_L = 0.895$) known, the footing rotation can be estimated using the procedures presented earlier. The first step is to predict footing uplift and the simple upper-bound limit from Equation 16 gives $M = 50$ kNm. Thus the footing will uplift before reaching the factored overturning capacity of $M = 86$ kNm. According to Equation 18, the maximum vertical load that results in the soil being linear at footing uplift is 224 kN. As the applied vertical load was 300 kN, the soil is nonlinear at footing uplift. Using Equation 14 for a more refined estimate of footing uplift, by solving for β at footing uplift, results in $\beta = 0.687$ and $q_{unf} = 437$ kPa, $q_{unf}/q_f = 0.624$, $M = 47.0$ kNm. This example suggests the extra effort is not warranted when the applied vertical load exceeds the limit in Equation 18 by 33%. $\xi_{NL} = 1.1$ from Figure 5 for the TL1 Winkler spring, which was used to make all predictions for the square footing on sand. $\theta = 0.00175$ at footing uplift from Equation 13.

The end of linear footing rotations can be determined using $P^* = 148$ kN from Equation 19 and substituting it into Equation 16 to give $M = 24.7$ kNm. The corresponding $\theta = 0.000825$ from Equation 13 with $\xi_{NL} = 1.0$ and $a = 0.667l_f$, $q_{unf} = 222$ kPa from Equations 9 and 10 for P^*. Footing uplift (UL) and end of linear range (EL) are indicated in Figure 6b along with the experimental data from Phase II with one large intermediate cycle of time history excluded for clarity. All data shown in Figure 6 are points along the envelope of cyclic response.

Equation 13 uses $G = 0.5G_0$ to predict the linear response until footing uplift or the soil becomes nonlinear. As shown in Figure 6a, that does not give a good prediction of foundation rotations at very small overturning moments, but as shown in Figure 6b, it does provide a very good estimate of the average rotations up to footing uplift. The footing rotations at very small overturning moments can be accurately estimated using Equation 13 by replacing the $0.5G_0$ term in Equation 13 with $1.0G_0$ and setting $\xi_{NL} = 1.0$.

Figure 6c compares the predicted rotations based on the TL1 Winkler springs with the Phase III test results. Also shown are the predicted rotations using linear springs (L) and bilinear springs (BL). A large part of the nonlinearity in footing overturning response is due to footing uplift and can be predicted with linear springs. For the square footings on sand, relatively little additional nonlinearity occurs due to soil response and the TL1 Winkler springs with a 50% reduction in slope ($m = 0.5$) provide an excellent prediction. When the footing is subjected to the factored overturning capacity of $M = 86$ kNm, the footing rotation is $\theta = 0.0062$.

NARROW FOOTINGS ON SILTY CLAY

Algie (2011) conducted field tests on a site in Auckland, New Zealand, with stiff cohesive soil formed by weathering of sandstone and siltstone. A 3.5 m-high steel frame was used to simultaneously load two 2.0 m-long by 0.4 m-wide by 0.4 m-deep concrete footings that were cast 6.0 m apart with the top of the footings at ground level. In the first phase of each test, the structure was subjected to low levels of forced vibration using an eccentric mass shaker. In the second phase, the structure was subjected to 9 or 10 cycles of monotonic lateral load that was slowly applied, but was instantly removed using a quick release to induce an impulsive excitation. The static load-deflection curves were measured during each pullback. The data from 9 cycles of one test, called Test 7, are examined here. The vertical load applied to the two footings was 260 kN. All predictions and results discussed below are for one footing; thus $P = 130$ kN.

Seismic down-hole tests were performed to depths of 3 m. Measured shear wave velocities varied (non-linearly) from 135 m/s to 196 m/s, and the density of soil was 1,700 kg/m^3. The calculated initial shear modulus varied from about 30,000 kPa to 65,000 kPa and had a mean value (from all data) of 41,000 kPa. Given that the 0.4 m-wide by 0.4 m-deep footings were at the surface, the lower-bound value of $G_0 = 30{,}000$ kPa was used similar to Algie (2011). Laboratory tests were performed on samples taken at a depth of 0.5 m. The average results: natural water content = 33%; plastic limit = 28; liquid limit = 54; and plastic index = 26.

The ultimate bearing strength can be determined from the measured overturning capacity of 100 kNm per footing. Rearranging Equation 8 gives $q_{unf} = q_{ult} = 700$ kPa. Thus $q_f = 350$ kPa, and the factored capacity of the footing is $M = 70$ kNm. Because the tests were conducted when the surface of the site was saturated with water, Poisson's ratio, ν, was assumed to be 0.49.

For the narrow footing subjected to a vertical load, causing a uniform bearing stress of about 50% of the factored bearing capacity, all predictions are made using the TL4 nonlinear Winkler springs, which have a 92% reduction in slope ($m = 0.08$) after reaching the linear limit. A discussion of how footing geometry influences nonlinear soil deformations and how to choose the Winkler springs or determine ξ_{NL} for the footing geometry and applied vertical load is presented after the comparison with experimental results.

According to Equation 16, the footing is expected to uplift when $M \geq 43.3$ kNm. Thus the footing will uplift before reaching the factored capacity of $M = 70$ kNm. According to Equation 18, the maximum vertical load that results in the soil being linear at footing uplift is 90 kN. Because the applied vertical load was 130 kN, the soil is predicted to be nonlinear prior to footing uplift. Solving for β and using Equation 14 to determine M at footing uplift results in: $\beta = 0.744$; $q_{unf} = 219$ kPa; $q_{unf}/q_f = 0.625$; and $M = 33.4$ kNm. In this case, when the TL4 Winkler springs are used and the applied vertical load is almost 50% larger than the linear limit, M at footing uplift from Equation 14 is 22% less than that from Equation 16. As the footing has a length-to-width ratio of $l_f/b_f = 5$ and a depth-to-length ratio of $d_f/l_f = 0.2$, $\xi_L = 0.249$ from Figure 1. At footing uplift, $\xi_{NL} = 1.49$ from Figure 5 and $\theta = 0.00066$ from Equation 13.

The end of linear footing response can be determined by solving for $P^* = 49.2$ kN from Equation 19 and substituting it into Equation 16 to determine $M = 16.4$ kNm. $\theta = 0.00021$ from Equation 13 with $\xi_{NL} = 1.0$, $a = 0.667 l_f$, and $q_{unf} = 92.2$ kPa. The predicted response using $G = 0.5G_0$ up to the end of the linear range (EL) and a simple linear interpolation between that point and the predicted footing uplift (UL) are shown in Figure 7a along with the experimental data from the first cycle of lateral loading. The measured initial rotational stiffness of the footing up to $M \leq 5$ kNm compares well with the prediction from Gazetas (1991) using $G = G_0$. The calculation of Gazetas' rotational stiffness can be made by substituting $\xi_L = 0.249$ from Figure 1 into Equation 4 and rearranging and solving for $K_\theta = 157{,}000$ kNm.

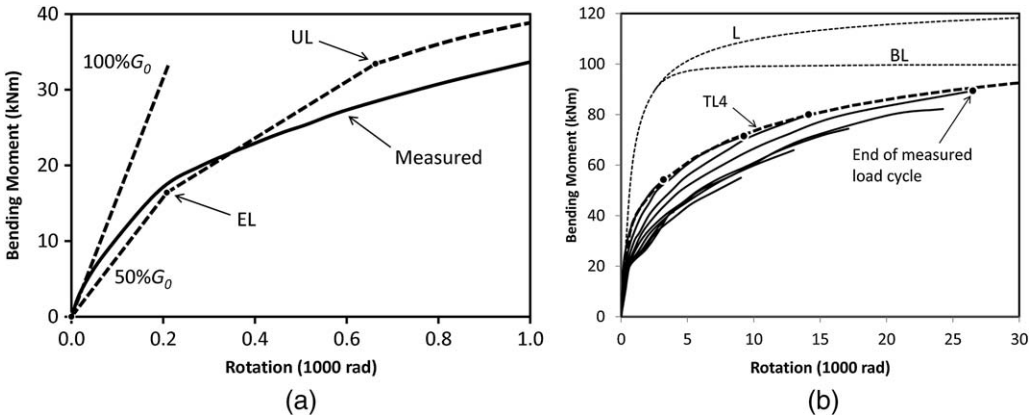

Figure 7. Comparison of predicted and observed rotations from tests of narrow footings on silty clay: (a) close up of first cycle, (b) all nine cycles of monotonic loading. Field test data from Algie (2011).

Figure 7b compares all of the measured field data from monotonic loading during one test (called Test 7) with the predicted rotations based on linear springs (L), bilinear springs (BL), and the TL4 springs. Unlike the square footings on sand, a significant portion of the footing rotation is due to nonlinear soil displacements, and the TL4 Winkler springs with a 92% reduction in slope ($m = 0.08$) provide an excellent prediction. When the footing is subjected to the factored overturning capacity of 70 kNm, the rotation is 0.0080.

SIMPLIFIED MODEL OF NONLINEAR SOIL DEFORMATIONS

The nonlinearity of the foundation moment-rotation relationship is due both to the uplift of the footing and the nonlinear stress-strain behavior of soil in compression. In some cases (e.g., Figure 6b), the nonlinearity is mostly due to footing uplift, while in other cases (Figure 7b), it is primarily the nonlinear soil deformations. The nonlinearity due to footing uplift is accounted for in Equation 13 by the ratio of footing length to the uniform bearing stress block length, l_f/a.

The first step in accounting for the nonlinear stress-strain behavior of soil is to develop a relationship between the soil strain and the displacement of the Winkler springs used to model the soil. Based on the results of field measurements of foundation settlements, load tests on model foundations, and plate loading tests, Atkinson (2000) showed that the effective stiffness of soil can be related to an "average strain" calculated as the foundation displacement divided by the foundation width. He showed that the effective stiffness of soil reduces with increasing "average strain" in the same way it does with increasing strain in a triaxial test, although a calibration factor is needed to relate "average strain" in a large foundation to the strains measured in a triaxial test.

The second step is to account for the difference in the nonlinearity of different soils. A lot has been learned since Seed and Idriss (1970) published their famous S-shaped curves for shear modulus degradation of sand; however, much of this knowledge is in the form of complex constitutive models that can only be applied in computer solutions. A number of investigators have recently developed simple empirical modulus reduction curves for different soils. For example, Oztoprak and Bolton (2013) developed new simplified curves for sand using a database of 454 tests from 65 references, while Vucetic and Dobry (1991) developed curves for fine-grained soil. These curves—and others available in the literature—can be used to relate the effective stiffness of soil to the soil strain. Because of the short deadline to complete the development for the 2015 Canadian building code, this step was not fully completed, and a simplified model was developed using an average shear modulus degradation, as described below. Information about the different properties of soil that influence the effective stiffness at medium-to-large strains will be provided in the commentary to the 2015 Canadian building code to allow adjustments to be made to the nonlinear soil factor, ξ_{NL}. The current draft includes: uniformity coefficient; relative density and mean effective stress for sands; and plasticity index for fine-grained soil.

The maximum soil displacement at the "toe" of a footing can be determined by rearranging Equation 11 to give $\Delta_{max} = c \cdot \theta$, which can also be expressed as $\Delta_{max} = a/\beta \cdot \theta$. Because β is fairly constant, this simplifies to $\Delta_{max} \propto a \cdot \theta$. At a given foundation rotation θ, the maximum soil displacement is proportional to the length of the uniform bearing stress distribution a. Thus it is proposed that a/b_f, which is proportional to the "average strain"

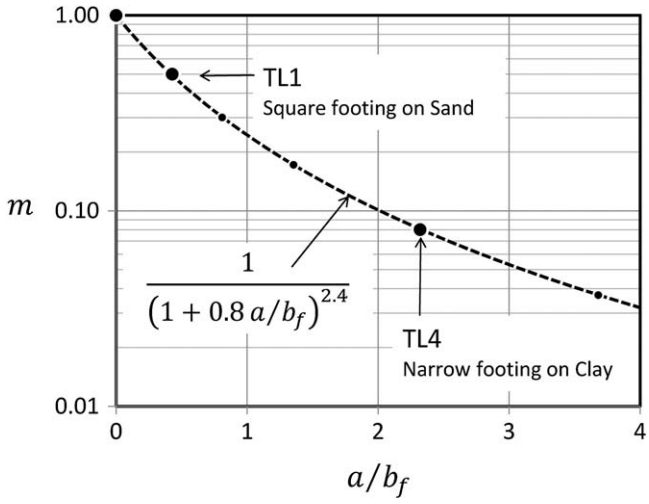

Figure 8. Proposed relationship between secondary slope of trilinear Winkler springs m and ratio of uniform bearing stress length to footing width a/b_f.

defined by Atkinson (2000), define which trilinear Winkler spring is appropriate to model the reduction in soil stiffness due to increasing soil strains. Figure 8 presents the proposed relationship between a/b_f and the slope of the second linear segment of the trilinear Winkler springs defined as m. The relationship was empirically developed based on the results of the tests described above and the requirement that as a/b_f approaches zero, the solution must be based on the linear Winkler spring ($m = 1.0$). Figure 9 presents a revised version of Figure 5 where ξ_{NL} is given as a function of both q_{unf}/q_f and a/b_f.

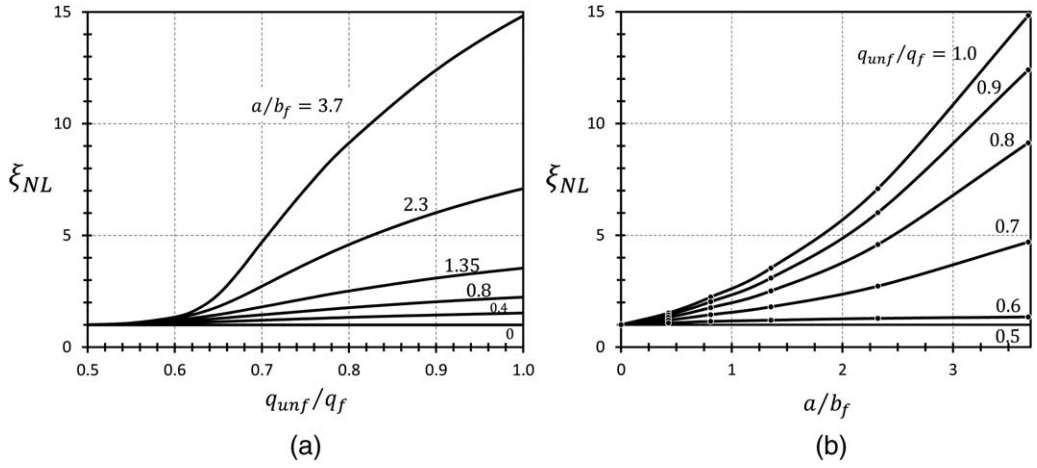

Figure 9. Non-dimensional parameter accounting for increased footing rotation due to nonlinearity of soil as a function of magnitude and length of required uniform bearing stress.

SUMMARY OF GENERAL METHOD AND SIMPLIFIED METHODS

The proposed general method for determining the rotation of a capacity-protected foundation subjected to an overturning moment equal to or larger than $M = P \cdot l_f/6$ is given by Equation 13. For smaller overturning moments, the foundation rotation can be estimated by assuming the moment – rotation relationship varies linearly from zero at $M = 0$, to the rotation given by Equation 13 when $M = P \cdot l_f/6$.

The parameters in Equation 13 include the magnitude and length of the uniform bearing stress required to resist the applied loads, given by Equations 9 and 10, and two non-dimensional parameters: ξ_L accounts for the initial linear rotational stiffness of the footing and is determined from Figure 1, and; ξ_{NL} accounts for the increased nonlinear rotation due to the reduction in shear modulus of soil with increasing soil strains and is determined from Figure 9. A simplified method results from using simpler estimates of ξ_L and ξ_{NL} when $q_{unf}/q_f \leq 1.0$. The resulting simplified method for estimating the rotation of a capacity-protected foundation subjected to an overturning moment equal to or larger than $P \cdot l_f/6$ is given by:

$$\theta = 0.2(1-\upsilon)\left(\frac{q_{unf}}{0.5G_0}\right)\left(\frac{l_f}{a}\right)\xi_L \cdot \xi_{NL} \tag{21}$$

$$\xi_L = \left(1 - 1.5\frac{d_f}{l_f}\right)\left(1 - 0.1\frac{l_f}{b_f}\right) \geq 0.2 \tag{22}$$

$$\xi_{NL} = 1 + 4\left(\frac{q_{unf}}{q_f} - 0.5\right)\left(\frac{a}{b_f}\right)^{1.5} \geq 1.0 \tag{23}$$

In Equations 22 and 23, $d_f/l_f \leq 0.4$; $l_f/b_f \leq 5$; $0.5 \leq q_{unf}/q_f \leq 1.0$.

The proposed simplified method given by Equations 21, 22, and 23 was used to predict the rotation of the test footings when subjected to their factored overturning capacity. When the square footing on sand is subjected to $M = 86\,\text{kNm}$, the simplified method predicts $\theta = 0.0071$, while the general method from Equation 13 with Figure 1 and Figure 9 gives $\theta = 0.0061$ similar to the test result. When the narrow footing on clay is subjected to $M = 70\,\text{kNm}$, the simplified method gives $\theta = 0.0145$, while the general method gives $\theta = 0.0080$, similar to the test. This demonstrates that while the simplified method provides a quick, safe estimate, the general method may give significantly less rotation.

An even simpler estimate of foundation rotation can be made by assuming $\xi_L = 1.0$ and $q_{unf}/q_f = 1.0$, resulting in the following equation that was adopted in 2014 CSA A23.3:

$$\theta = 0.15\left(\frac{q_{unf}}{0.5G_0}\right)\left(\frac{l_f}{a}\right)\left\{1 + 2\left(\frac{a}{b_f}\right)^{1.5}\right\} \tag{24}$$

Equation 24 is given in Clause 21.10 on foundation design in 2014 CSA A23.3, while Equations 21, 22, and 23, as well as Figures 1 and 9, are provided in the commentary as more refined methods for estimating foundation rotation. In addition, information is provided

about the different properties of soil that influence the effective stiffness at medium to large strains to allow adjustments to be made to the nonlinear soil factor, ξ_{NL}.

DESIGN OF FOUNDATIONS FOR REDUCED ROTATION

With the simple methods presented above, a structural engineer can quickly estimate the rotation of a capacity-protected shear wall foundation and thus can design the foundation for improved performance rather than just strength. The concept is demonstrated by two examples.

The soil properties are from a high-rise building site where the soil was classified as very dense glacial till based on test-hole information. The factored bearing capacity for (transient) earthquake loads is 1200 kPa and Poisson's ratio of soil is 0.2. Shear wave velocities were measured at 1 m increments to a depth of 39 m. Based on the data within 15 m of the foundation, the average shear wave velocity of the soil is about 500 m/s. Using a mass density of 2,000 kg/m^3, the initial shear modulus $G_0 = 500{,}000$ kPa.

The first example is the core footing for a 30-story building with a 7.5 m × 7.5 m central shear wall core. The weight of the shear walls and tributary areas of supported slabs results in a total vertical force of $P = 64{,}500$ kN applied to the core footing, and the axial compression in the individual wall piers plus the vertical reinforcement in the walls results in a total nominal overturning capacity of the shear wall core of $M = 377{,}400$ (note: $M/P = 5.85$ m). A square footing with $l_f = 14.3$ m, $b_f = 14.3$ m, and $d_f = 2.4$ m has a factored overturning capacity equal to the nominal capacity of the shear walls. The total vertical force applied to the soil, including the footing self-weight, is 76,200 kN. The required eccentricity of the soil reaction force is 4.95 m, and the required length of uniform bearing stress given by Equation 9 is $a = 4.43$ m with $q_{unf} = q_f = 1{,}200$ kPa. Equation 24 gives $\theta = 0.0031$ to develop the factored overturning capacity of the footing. Equation 22 gives $\xi_L = 0.672$, Equation 23 gives $\xi_{NL} = 1.344$, and Equation 21 gives $\theta = 0.0022$. While this is a relatively small rotation, the building has multiple levels below grade and the shear walls are interconnected to other concrete walls by multiple floor diaphragms that have high in-plane stiffness prior to cracking. A small footing rotation may result in considerable redistribution of the seismic shear to other walls below grade. Rad and Adebar (2009) presented a method for designing the shear walls accounting for footing rotations, as well as cracking of diaphragms and cracking of shear walls.

In the second example, a more lightly loaded shear wall footing is designed for the same site. A 20-story building has two smaller shear wall cores rather than a large central core. One of the cores, formed by the walls around a stairwell, is 7.1 m × 2.75 m in plan. With the reduced building height, thinner concrete walls and smaller slab tributary areas due to the core being at the end of the building, the vertical force applied to the footing is only $P = 12{,}850$ kN and the nominal overturning capacity of the shear walls is $M = 110{,}670$ kNm. With $M/P = 8.61$ m, a fairly large footing is needed to resist the overturning moment. A rectangular footing with $l_f = 13.6$ m, $b_f = 9.0$ m and $d_f = 2.0$ m provides the required overturning strength. The total vertical force applied to the soil is 18,610 kN and the required eccentricity of the soil reaction force is 5.95 m. The required length of uniform bearing stress given by Equation 9 is $a = 1.724$ m, with $q_{unf} = q_f = 1{,}200$ kPa. Equation 24 gives $\theta = 0.0066$ to develop the factored overturning capacity.

Equation 22 gives $\xi_L = 0.662$, Equation 23 gives $\xi_{NL} = 1.168$, and Equation 21 gives $\theta = 0.0047$. The footing rotation is increased from the first example because of the reduced bearing stress length resulting from the smaller vertical load. Note that l_f/a equals 3.24 in the first example and 7.91 in the second example.

The sizes of the two footings, which were designed to meet the strength requirement, were increased to investigate how much footing size influences footing rotations. For the square footing, the length and width of the footing were increased equally, while the depth was kept constant. For the rectangular footing, only the length was increased. This was done to make the two examples realistic even though it makes them more difficult to compare. As construction costs are proportional to concrete volume, the results are summarized in Figure 10 in terms of footing volume relative to the minimum strength requirement.

When the moment applied to a footing is constant and the footing length is increased, the eccentricity of the soil reaction force (from the resultant of the vertical load applied to the footing) reduces because of the increased weight of footing. The change in location of the soil reaction force and the increased footing length both contribute to an increase in length of the uniform bearing stress. The increase in a, and the resulting reduction of q_{unf}, directly reduce the rotations determined from Equations 13, 21, or 24. The reduction in q_{unf} has an additional indirect effect by reducing ξ_{NL} when using Equations 13 or 21.

For one of the example footings—the lightly loaded rectangular footing—increasing the footing size quickly reduces the rotations required to develop the factored overturning moment. Increasing the footing length from 13.6 m to 14.2 m (4% increase in volume) reduced the rotation by 50% from 0.0047 to 0.0023, while increasing the length to 15 m

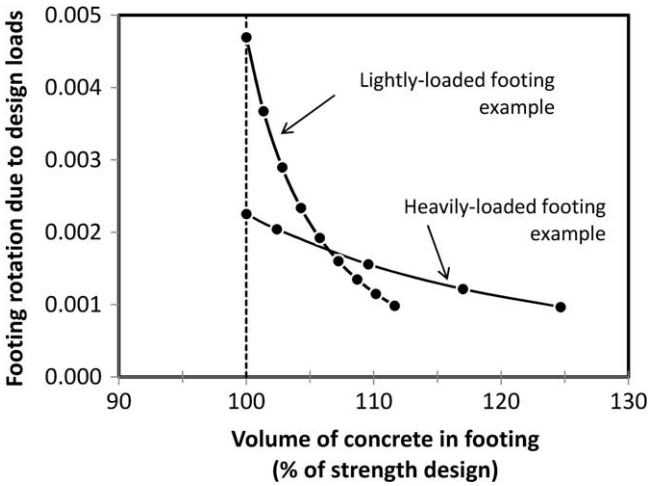

Figure 10. Results of two footing design examples showing the reduction of footing rotation due to increased footing size relative to the minimum strength requirement for a lightly loaded rectangular footing and a heavily loaded square footing.

(10% total increase in footing volume) reduced the rotation by 75% to 0.0011. The small additional cost to increase the footing size will greatly improve the building performance when subjected to the design earthquake due to the smaller demands on the gravity load–resisting structure.

CONCLUSIONS

A simple hand-calculation method has been developed for estimating the amount that a capacity-protected foundation will rotate when subjected to a large overturning moment such as the capacity of the SFRS. The method comes in three forms: a general procedure that requires two non-dimensional parameters to be determined from figures, a simpler version that gives larger estimates of rotation because the two parameters are estimated from approximate linear equations, and finally, a very simplified procedure that consists of a single equation. This simplified equation has been adopted into CSA A23.3-2014, which is a part of the 2015 Canadian building code. While the method was developed for estimating the nonlinear rotations due to large overturning moments, it can also be used to accurately determine linear rotations due small overturning moments by setting $\xi_{NL} = 1.0$ and replacing the $0.5G_0$ term in Equation 13 with $1.0G_0$, or any other effective shear modulus as given in ASCE 41-06.

The developments that permit a simple hand-calculation method are: (1) expressing the linear rotational stiffness of a footing in terms of a non-dimensional parameter ξ_L given by Equation 4 and Figure 1; (2) converting complex nonlinear bearing stress distributions into statically equivalent uniform bearing stress distributions; and (3) relating the soil displacement at the "toe" of a footing, accounting for nonlinearity of soil, to the magnitude of statically equivalent uniform bearing stress using the non-dimensional parameter ξ_{NL} given in Figure 9.

The proposed hand-calculation method accounts for nonlinearity due to footing uplift in a rigorous way and, therefore, generally gives a good estimate of footing rotation when most of the rotation is due to footing uplift—for example, in footings with a high factor of safety against bearing failure due to vertical (gravity) loads. While structural engineers often ignore the movement of such foundations, significant rotation may be required to develop the concentrated bearing stresses at the footing "toe." Estimating the additional footing rotation that occurs because of the degradation of soil stiffness at medium to large strains is a complex task. Using an average stiffness degradation, the proposed method focuses on the relationship between displacement at the footing "toe" and the average soil strain that influences the stiffness degradation. The difference in nonlinearity of different soils can be accounted for by adjusting the effective shear modulus used in the method, that is, replacing the $0.5G_0$ term in Equations 13, 21, or 24, depending on the level of average strain and the properties of the particular soil. As a larger portion of the footing rotation is from the nonlinearity of soil in compression, the accuracy of the proposed method reduces. Future developments will focus on this limitation.

Design examples illustrate how the proposed simple method for estimating foundation rotation allows the structural engineer to design the foundation for significantly improved performance (reduced rotations) at small additional cost. All test predictions and design examples were presented with sufficient detail so the reader can reproduce all numbers.

ACKNOWLEDGMENTS

The author is grateful for the many invaluable contributions by Dr. Ronald DeVall of Read Jones Christoffersen; the helpful input provided by colleagues Professors Donald Anderson, Liam Finn, and John Howie; the review of the proposal for the 2015 Canadian building code by the seismic design group of CSA Technical Committee A23.3; as well as the helpful comments provided by the technical reviewers of *Earthquake Spectra*.

REFERENCES

Adebar, P., Bazargani, P., Mutrie, J., and Mitchell, D., 2010. Safety of gravity-load columns in shear wall buildings designed to Canadian standard CSA A23.3, *Can. J. Civ. Eng.* **37**, 1451–1461.

Algie, T. B., 2011. Nonlinear Rotational Behaviour of Shallow Foundations on Cohesive Soil, Ph.D. Thesis, University of Auckland, New Zealand.

Allotey, N., and El Naggar, M. H., 2003. Analytical moment–rotation curves for rigid foundations based on Winkler model, *Soil Dyn. and Earthquake Eng.* **23**, 367–381.

American Society of Civil Engineers (ASCE 41–06), 2007. Seismic Rehabilitation of Existing Buildings, *ASCE Standard ASCE/SEI 41–06*, Reston, VA.

Atkinson, J. H., 2000. Non-linear soil stiffness in routine design, *Géotechnique* **50**, 487–508.

Bazargani, P., 2014. Seismic Demands on Gravity-Load Columns of Concrete Shear Wall Buildings, Ph.D. Thesis, University of British Columbia, Canada.

Boulanger, R. W., Curras, C. J., Kutter, B. L., Wilson, D. W., and Abghari, A., 1999. Seismic soil-pile-structure interaction experiments and analyses, *J. Geotech. and Geoenv. Eng.*, ASCE, **125**, 750–759.

Canadian Standards Association (CSA), 2014. *Design of Concrete Structures*, CSA A23.3-14, Rexdale, ON, Canada.

Gajan, S., Kutter, B. L., Phalen, J. D., Hutchinson, T. C., and Martin, G. R., 2005. Centrifuge modeling of load-deformation behavior of rocking shallow foundations, *Soil Dyn. and Earthquake Eng.* **25** 773–783.

Gazetas, G., 1991. Foundation vibrations, *Foundation Engineering Handbook*, H. Y. Fang, ed., 2nd Edition, Van Nostrand Reinhold, New York, 553–593.

Gazetas, G., and Mylonakis, G., 1998. Seismic soil-structure interaction: new evidence and emerging issues, *Soil Dynamics III*, ASCE Special Geotechnical Publication, Vol. **2**, 1119–1174.

Negro, P., Verzeletti, G., Molina, J., Pedretti, S., Lo Presti, D., and Pedroni, S., 1998. Large-scale geotechnical experiments on soil–foundation interaction, *Special Publication No. I.98.73*, Joint Research Center, European Commission, Ispra, Italy.

Oztoprak, S., and Bolton, M. D., 2013. Stiffness of sands through a laboratory test database, *Géotechnique* **63**, 54–70.

Pais, A., and Kausel, E., 1988. Approximate formulas for dynamic stiffnesses of rigid foundations, *Soil Dyn. and Earthquake Eng.* **7**, 213–227.

Pender, M. J., Algie, T. B., Storie, L. B., and Salimath, R., 2013. Rocking controlled design of shallow foundations, *Proc. of 2013 NZSEE Conf.*, Wellington, New Zealand.

Rad, B. R., and Adebar, P., 2009. Seismic design of high-rise concrete walls: reverse shear due to diaphragms below flexural hinge, *J. of Struct. Eng.* **135**, 916–924.

Seed, H. B., and Idriss, I. M., 1970. *Soil Moduli and Damping Factors aor Dynamic Response Analyses*, Report EERC 70–10, University of California, Berkeley.

Vijayvergiya, V. N., 1977. Load-movement characteristics of piles, *Proceedings, Ports 77: 4th Annual Symposium of the Waterway, Port, Coastal, and Ocean Division of ASCE*, Long Beach, CA, 269–284.

Vucetic, M., and Dobry, R., 1991. Effect of soil plasticity on cyclic response, *J. Geotech. Eng.*, ASCE, **117**, 89–107.

Yan, L. P., and Martin, G. R., 1999. Simulation of moment–rotation behavior of a model footing, in *Proc. of Int. FLAC Symp. on Num. Mod. in Geomechanics*, Minneapolis, MN, 365–370.

(Received 28 January 2014; accepted 27 October 2014)